THE ROYAL SOCIETY

Published online 3 October 2002

Electron, proton and hydrogen-atom transfers in photosynthetic water oxidation

Cecilia Tommos

Department of Biochemistry and Biophysics, Arrhenius Laboratories for Natural Sciences, Stockholm University, SE-106 91 Stockholm, Sweden (*cecilia@dbb.su.se*)

When photosynthetic organisms developed so that they could use water as an electron source to reduce carbon dioxide, the stage was set for efficient proliferation. Algae and plants spread globally and provided the foundation for our atmosphere and for O_2-based chemistry in biological systems. Light-driven water oxidation is catalysed by photosystem II, the active site of which contains a redox-active tyrosine denoted Y_Z, a tetramanganese cluster, calcium and chloride. In 1995, Gerald Babcock and co-workers presented the hypothesis that photosynthetic water oxidation occurs as a metallo-radical catalysed process. In this model, the oxidized tyrosine radical is generated by coupled proton/electron transfer and re-reduced by abstracting hydrogen atoms from substrate water or hydroxide-ligated to the manganese cluster. The proposed function of Y_Z requires proton transfer from the tyrosine site upon oxidation. The oxidation mechanism of Y_Z in an inhibited and O_2-evolving photosystem II is discussed. Domino-deprotonation from Y_Z to the bulk solution is shown to be consistent with a variety of data obtained on metal-depleted samples. Experimental data that suggest that the oxidation of Y_Z in O_2-evolving samples is coupled to proton transfer in a hydrogen-bonding network are described. Finally, a dielectric-dependent model for the proton release that is associated with the catalytic cycle of photosystem II is discussed.

Keywords: photosystem II; photosynthetic water oxidation; oxygen-evolving complex; redox-active tyrosine; tyrosine radical

1. INTRODUCTION

PSII catalyses the light-driven oxidation of water to molecular oxygen in plants, algae and cyanobacteria. Detailed structural information on this large, membrane-bound pigment–protein complex is emerging. Zouni *et al.* (2001) reported a 3.8 Å resolution X-ray crystal structure of PSII from the thermophilic cyanobacterium *Synechococcus elongatus*. Barber and his collaborators have used cryoelectron microscopy, and single particle analysis, to derive three-dimensional structural maps of PSII from several oxygenic organisms (see Nield *et al.* (2002) and references therein). PSII contains more than 25 subunits and is located in the thylakoid membrane of chloroplasts and cyanobacteria. The reaction-centre core is composed of the D1 and D2 proteins, which bind the cofactors that are involved in the primary photochemistry and the secondary electron-transfer reactions. In direct association with the D1/D2 heterodimer are the chlorophyll *a*-containing CP43 and CP47 inner antenna proteins, which funnel excitation energy to the reaction centre. Photosystem II in higher plants and green algae has an outer antenna system of chlorophyll *a*/*b*-containing proteins that include LHCII, CP24, CP26 and CP29. In addition, the catalytic site is protected by three extrinsic proteins that are bound to the enzyme on the lumenal side of the thylakoid membrane.

Catalysis is initiated by photo-oxidation of the reaction-centre chlorophyll species P_{680} followed by rapid reduction of the Q_A quinone via a pheophytin (Diner *et al.* 2001). The P^+_{680}/Q^-_A charge-separated state is stabilized on the acceptor side of PSII by electron transfer to the second quinone Q_B. On the donor side of PSII, P^+_{680} is reduced by the Y_Z tyrosine located in position D1-161 (Babcock *et al.* 1989; Tommos & Babcock 2000). The tyrosine radical is re-reduced by a cluster of four manganese ions (Dau *et al.* 2001; Peloquin & Britt 2001; Robblee *et al.* 2001; Carrell *et al.* 2002). The manganese cluster binds substrate water (Hillier & Wydrzynski 2000) and, by cycling through five different redox states, denoted the S-states, accumulates the oxidizing potential required for the catalytic process. Following the absorption of four photons, the enzyme reaches the S_4-state upon which oxidation of water occurs along a concerted pathway and dioxygen is released as the system resets to S_0. Calcium and chloride are required for catalysis and are generally believed to be associated with the manganese centre (Wincencjusz *et al.* 1997; Robblee *et al.* 2001; Carrell *et al.* 2002). PSII also contains Y_D, a second redox-active tyrosine located at position D2-160 (Babcock *et al.* 1989). Y_D serves as an auxiliary electron donor and is not directly involved in the main electron-transport chain.

2. THE HYDROGEN-ATOM ABSTRACTION MODEL

The focus of this paper is on Y_Z and its functional role in the unique water-oxidizing process catalysed by PSII. Seven years ago, Gerald T. Babcock and co-workers

One contribution of 21 to a Discussion Meeting Issue 'Photosystem II: molecular structure and function'.

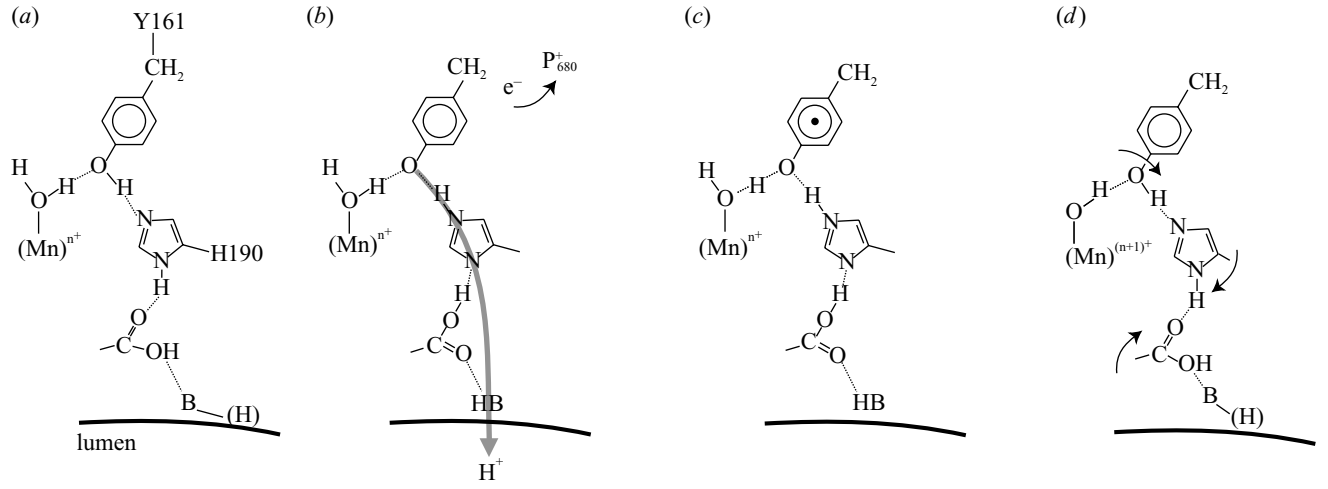

Figure 1. Proton-transfer reactions associated with the oxidation and reductions of Y_Z as proposed by Babcock and co-workers. (*a*) Functional organization of the active site in the dark. (*b*) Reduction of P^+_{680} coupled with domino-deprotonation of Y_Z via an hydrogen-bonded chain/web extending from the tyrosine towards the exterior of the protein and the bulk solution. (*c*) Proton-coupled electron transfer from the manganese/substrate centre to the $Y_Z^{\cdot}$ radical. (*d*) Resetting of the proton-transfer pathway leading from the tyrosine site.

presented the hypothesis that photosynthetic water oxidation occurs as a metallo-radical catalysed process (Babcock 1995; Hoganson *et al.* 1995; Tommos *et al.* 1995). This new conceptual model for PSII involved Y_Z directly in the deprotonation and oxidation of substrate water, as described in figure 1 (see also Gilchrist *et al.* 1995). In the dark, Y_Z was proposed to be hydrogen-bonded to D1-H190 and to a manganese-ligated substrate molecule. Following light absorption, Y_Z reduces P^+_{680} and transfers its phenolic proton to D1-H190. The histidine, in turn, transfers a proton to a second acceptor and a domino-deprotonation occurs that eventually gives rise to the release of one proton into the thylakoid lumen. The neutral $Y_Z^{\cdot}$ radical oxidizes the manganese cluster and simultaneously deprotonates substrate water/hydroxide ligated to the metal site. The proton-transfer pathway from the tyrosine site towards the protein exterior and the bulk phase is reset and the cycle is completed. The proton-coupled electron-transfer function for Y_Z illustrated in figure 1 provided the foundation for the hydrogen-atom abstraction model in which Y_Z was postulated to perform the same function on all S-state transitions. The essence of this model is that one substrate proton is transported from the active site towards the lumen and one oxidizing equivalent is transported from P^+_{680} to the manganese cluster, per Y_Z redox cycle. The metal site accumulates oxidizing potential and substrate oxidation occurs as a concerted reaction in the final $S_3 \rightarrow S_4 \rightarrow S_0$ transition. The basic proton-coupled electron-transfer events described in figure 1 have been incorporated into other mechanistic models for PSII (Pecoraro *et al.* 1998; Haumann & Junge 1999; Siegbahn 2000; Vrettos *et al.* 2001).

One attractive feature of the H-atom abstraction model is that the active site remains electroneutral throughout the catalytic cycle. This is consistent with thermodynamic considerations on photosynthetic water oxidation that suggest that the reduction potentials of both Y_Z and the manganese cluster must remain essentially invariant over the S-state cycle (Pecoraro *et al.* 1998; Tommos & Babcock 2000). In the H-atom abstraction model, only one pathway is required to transport substrate protons from the active site to the lumen. Mechanistically, the transfer is driven by the large ΔpK of the reduced versus oxidized tyrosine. This mode of substrate proton delivery rationalizes the observation that the majority of protons released from PSII during the catalytic cycle can appear in the bulk phase on the level of $Y_Z^{\cdot}$ and before oxidation of the manganese cluster (Haumann & Junge 1994; Bögershausen & Junge 1995). No other substrate proton-transfer pathways have yet, to our knowledge, been identified or suggested for PSII. The thermodynamic and kinetic competence and various other aspects of the H-atom abstraction model have been described elsewhere (see Hoganson & Babcock (2000); Tommos & Babcock (2000) and references therein).

A key step in the reaction sequence described in figure 1 is the net proton transfer from the tyrosine site towards the protein exterior and the thylakoid lumen upon oxidation of Y_Z. Many studies have been performed to characterize the proton-coupled electron-transfer reactions that are associated with the redox-active tyrosines in PSII. The results from these studies are summarized below and discussed within the framework of the mechanism depicted in figure 1.

3. THE REDOX PROPERTIES OF Y_D

During the 1980s, Babcock and co-workers used specific isotopic labelling combined with CW-EPR spectroscopy to show that Y_D and Y_Z were tyrosines. This study was followed by site-directed mutagenesis work, which identified Y_D as D2-Y160 and Y_Z as D1-Y161 (Babcock *et al.* 1989). FTIR spectroscopy and a variety of CW and pulsed EMR techniques have been used to investigate the protonation state and hydrogen bonding of Y_D in its reduced and oxidized form. Hienerwadel *et al.* (1997) showed that reduced Y_D is protonated and H-bonded to a neutral histidine at pH 6.0. The vibrational

modes of Y_D and $Y_D^{\cdot}$ were perturbed in a *Synechocystis* D2-H189Q mutant, which indicated that H-bonding occurs between D2-H189 and the tyrosine in both of its redox states. Britt and co-workers showed conclusively that $Y_D^{\cdot}$ is H-bonded to D2-H189 by using electron spin echo–electron nuclear double resonance spectroscopy combined with samples prepared from ^{15}N-labelled wild-type and D2-H189Q (Campbell *et al.* 1997). The number of H-bonding partners to $Y_D^{\cdot}$ varies in different organisms. EMR data representing $Y_D^{\cdot}$ in H_2O/D_2O-exchanged samples from spinach are best simulated by one exchangeable deuteron within H-bonding distance, while equivalent data of $Y_D^{\cdot}$ in *Synechocystis* are best described by two exchangeable deuterons (Force *et al.* 1995; Diner *et al.* 1998; Diner 2001). The Y_D site is deeply buried and H_2O/D_2O exchange occurs on the tens of hours time-scale (Babcock *et al.* 1989; Diner *et al.* 1998; Tommos *et al.* 1998*b*). A well-protected site is consistent with the remarkable stability of the radical, which decays on the hour time-scale at neutral pH (Vass & Styring 1991). EMR characterization of $Y_D^{\cdot}$ in a variety of samples including apo-PSII, calcium-depleted, acetate-treated, ammonia-treated and fully active samples from different oxygenic organisms show hyperfine coupling patterns and spectral features that are consistent with a neutral radical residing in a well-ordered environment (Rigby *et al.* 1994*a*,*b*; Warncke *et al.* 1994). These data reflect the asymmetry in PSII with respect to the position of the manganese cluster relative to Y_D and Y_Z (Zouni *et al.* 2001). As will be described in detail in §§ 5 and 8, Y_Z is greatly affected by the state of the manganese centre.

In a recent elegant study by Rutherford and co-workers, Y_D oxidation was shown to occur with a half-time of *ca.* 190 ns at pH 8.5 in apo-PSII (Faller *et al.* 2001). This rapid oxidation rate was observed in *ca.* 50% of the PSII centres and decreases to a time-scale of hundreds of microseconds at lower pH. At pH 8.5, the oxidation rates of Y_D and Y_Z are similar, but at pH 6.5 the oxidation of the former is much slower. This is an interesting observation since Y_D sits deeply buried in a well-ordered protein environment, while Y_Z in apo-PSII resides in a disordered site in rapid exchange with the bulk solvent (see § 5 below). The differences in oxidation rates at lower pH may be related to how the system manages the phenolic protons that are released upon oxidation of the tyrosines. Proton-transfer reactions that are coupled to the oxidation of Y_Z will be discussed in detail below. Less is known about the protonic reactions that are coupled to the oxidation of Y_D. The oxidation of Y_D and Y_Z induce shifts in the optical spectrum of P_{680}. These spectral band-shifts have been interpreted to be of electrochromic origin and thus to arise from charge accumulation in the protein upon oxidation of the tyrosines. This interpretation is controversial since the optical band-shifts may arise from electrostatic events or from structural effects (see Tommos *et al.* 1998*a*; Diner *et al.* 2001). The charge issue is relevant for discussions on the function of Y_D. Faller *et al.* (2001) proposed a model in which a charge present in the Y_D, site increases the reduction potential of P_{680}^+/P_{680} and shifts the positive charge of P_{680}^+ towards the D1 side, thereby making the oxidation of Y_Z more efficient. This model predicts that the oxidation rate of Y_Z should be sensitive to the absence or presence of Y_D, particularly since distance is the main parameter that determines electron-tunnelling rates in proteins (Page *et al.* 1999). In contrast to this prediction, the rate of Y_Z oxidation is the same in a Y_D-less mutant as in wild-type containing oxidized $Y_D^{\cdot}$ (Hays *et al.* 1999), as pointed out by the authors themselves (Faller *et al.* 2001). A second interesting suggestion made recently is that Y_D may be involved in the photoassembly of the manganese cluster (Ananyev *et al.* 2002).

In conclusion, a wealth of new information on Y_D has emerged. Whether the protonic charge remains close to $Y_D^{\cdot}$ or if it is transported out of the protein, and how these different scenarios may be coupled to function, however, need further investigations. The protonic events that are coupled to Y_Z oxidation in apo-PSII have been characterized in some detail and are described below.

4. THE p*K* VALUES OF Y_Z AND ITS PROTON ACCEPTOR IN APO-PSII

By analogy with the Y_D of the D2 protein, the oxidation of Y_Z has been linked to D1-H190. Diner, Sayre, Debus and their respective co-workers have made and characterized a series of D1-H190 mutants (see Debus (2001) and references therein). Only in the case of the D1-H190R and D1-H190K site-directed mutants, in which the histidine is replaced by another basic residue, did the assembly of a functional $(Mn)_4$-cluster occur resulting in a small fraction of PSII centres able to evolve oxygen at a low rate. At neutral pH, the rate of the $Y_Z \rightarrow P_{680}^+$ electron-transfer reaction was slowed more than 10^3 times in all D1-H190 mutants investigated. The oxidation efficiency of Y_Z was enhanced by raising the pH, or by the addition of imidazole or other bases small enough to access the tyrosine site and functionally substitute D1-H190. In the absence of the manganese cluster, the reduction of $Y_Z^{\cdot}$ is slow in the D1-H190 mutants relative to the wild-type, although the reduction rate can be increased substantially by the addition of small exogenous bases. These data suggest that D1-H190 is involved in both the deprotonation reaction of Y_Z upon oxidation and the reprotonation event coupled to the reduction of $Y_Z^{\cdot}$ in apo-PSII.

In order to understand the redox cycle of Y_Z, it is important to determine the p*K* of the tyrosine and its H-bonding partner(s) and how these values may change under various conditions. Diner *et al.* (1998) measured the oxidized–reduced difference spectra of Y_Z at pH 9.0 and 6.1 in apo-PSII and compared the pH 9 – 6.1 double-difference spectrum with an equivalent spectrum obtained from tyrosine in water. Assuming that the extinction coefficients are the same in PSII as in water, and that the radical spectrum is pH-independent, the authors concluded that *ca.* 60% of Y_Z is deprotonated at pH 9.0. This corresponds to a pK_{RED} of 8.6, which is lower than the value derived by Debus and co-workers (Hays *et al.* 1999) on comparable *Synechocystis* samples. The reduction of P_{680}^+ was measured in a D1-H190A mutant as a function of pH. The percentage of PSII centres with rapid Y_Z oxidation increased steeply at alkaline pH, suggesting direct titration of the tyrosine. An apparent p*K* of 10.3 was derived from the titration data and the authors proposed that this value

corresponds to pK_{RED} of Y_Z in the mutant. Styring and co-workers measured the light-induced chlorophyll *a* fluorescence in two dark-grown D1-H190 mutants from *Chlamydomonas reinhardii* (Mamedov *et al.* 1998). The induction of fluorescence, which is sensitive to the $Y_Z \rightarrow P_{680}^+$ electron-transfer reaction, showed a pH dependence with a pK of 8.1, and this value was assigned to Y_Z. Hays *et al.* (1999) have argued that the value of 8.1 is too low and estimated a pK closer to 9 from the fluorescence data. From the work described above, it is concluded that pK_{RED} of Y_Z is in the range of 8.6–10.3 in apo-PSII.

Using time-resolved optical spectroscopy, Conjeaud & Mathis (1980) reported that the rate of P_{680}^+ reduction in Mn-depleted PSII is strongly influenced by the bulk pH. Two more recent studies have reinvestigated the pH-dependence of the P_{680}^+ reduction kinetics in apo-PSII (Ahlbrink *et al.* 1998; Hays *et al.* 1999). In both of these studies, the reduction of P_{680}^+ was shown to be multiphasic. The amplitudes of the various kinetic phases were strongly modulated by the pH, while the rate constants were only weakly pH-dependent. This is indicative of a situation in which the proton equilibria are slow relative to the observed electron-transfer reaction. The multiple kinetic phases correspond to different protonation states, the relative populations of which are modulated by the bulk pH. In this case, the derived pKs represent the system in the dark before light excitation. Ahlbrink *et al.* (1998) studied the pH-dependence of P_{680}^+ reduction in salt-containing PSII core samples prepared from pea and derived an apparent pK of 7.0. The authors propose that this pK represents either Y_Z, or the base that accepts the phenolic proton upon oxidation of the tyrosine. Hays *et al.* (1999) studied PSII core particles from a D1-H190A *Synechocystis* mutant and demonstrated that the pK of Y_Z oxidation follows the solution pKs of the externally added bases. They concluded from these measurements that the pH profile of Y_Z oxidation reflects the pK of the base that accepts the phenolic proton and assigned a pK of 7.5 for D1-H190 in the wild-type. This value was shown to be sensitive to the salt concentration in the buffer and decreased to 6.9 in the presence of $CaCl_2$ and $MgCl_2$. The results from the optical work are consistent with the fluorescence study by the Styring group, who assigned a pK of 7.6 for D1-H190 in *C. reinhardii* (Mamedov *et al.* 1998). The latter study was performed with no Ca^{2+} and Mg^{2+} ions in the sample buffer. Thus, the pK assigned to D1-H190 is very similar for PSII prepared from cyanobacteria, algae and higher plants and decreases by about half a pK unit in the presence of salt. In one study, the pK linked to the $Y_Z \rightarrow P_{680}^+$ electron-transfer reaction was reported to be 8.3 (Diner *et al.* 1998), but this value may arise from the deconvolution of low time-resolution data (Hays *et al.* 1999).

Two groups have investigated the rate of $Q_A^-/Y_Z^{\cdot}$ recombination as a function of pH in apo-PSII. Both groups reported monophasic kinetics, suggesting fast proton equilibria relative to the observed reaction, which is slow and occurs on the millisecond time-scale. In this case, the measured pK represents the base during the reaction and, thus, in the presence of $Y_Z^{\cdot}$. Rappaport & Lavergne (1997) characterized the system optically and reported a pK of *ca.* 6.0 for both core particles from *C. reinhardii* and PSII-enriched membranes from spinach. The salt dependence was investigated in the membrane samples and the pK was shown to decrease to 5.1 upon the addition of $MgCl_2$. Mamedov *et al.* (1998) studied the pH-dependence of the recombination rate by flash-induced fluorescence decay and derived a similar pK of 6 in the absence of salt (see also Rappaport & Lavergne 2001; F. Mamedov, personal communication). It was proposed that this pK represents the distal nitrogen of D1-H190 after protonation of the histidine nitrogen proximal to Y_Z upon radical formation (Rappaport & Lavergne 1997; Mamedov *et al.* 1998).

The pK values assigned to Y_Z and D1-H190 at various conditions are summarized in figure 2. The figure also describes proton-transfer reactions that are proposed to follow the oxidation of the tyrosine. Y_Z has a pK in the range 8.6–10.3, which brackets the 9.9 value for tyrosine in water (Tommos *et al.* 1999). As described above, the 7.0 (salt) and 7.5 (no salt) pK values represent D1-H190 in the dark before light excitation. Figure 2*a* illustrates Y_Z oxidation at a pH above the pK of D1-H190 in the presence of reduced Y_Z. At high pH, the histidine is neutral and in H-bonding contact with Y_Z. The connection between the tyrosine and the histidine can occur via a single H-bond, as shown in figure 2, or indirectly via a water bridge (Diner *et al.* 1998; Hays *et al.* 1999; Debus 2001; Diner 2001) or other residues. EMR data have shown that $Y_Z^{\cdot}$ is a neutral, deprotonated radical at pH 6.0 (Tommos *et al.* 1995). The pK of Y_Z in its oxidized state is expected to be very low. The pK_{OX} of phenol is *ca.* -2 in water and decreases even further in solvents with lower dielectric constants (Dixon & Murphy 1976; Bordwell & Cheng 1991). As indicated by the work described above, the pK of the H-bonding partner to Y_Z is sensitive to its redox state and drops with 1.5–2 pK units upon oxidation of the tyrosine. Thus, the pK values of 5.1 (salt) and 6.0 (no salt) represent D1-H190 in the presence of $Y_Z^{\cdot}$. It should be noted that the pK values assigned to D1-H190 may represent global pKs that involve several connected residues in addition to the histidine. For simplicity, only H190 is shown as the acceptor for the phenolic proton in figure 2, but more complex structures are possible.

The following events are proposed to occur in apo-PSII upon light excitation. As Y_Z becomes oxidized, its phenolic proton is transferred to D1-H190, which in turn deprotonates at its distal nitrogen. In this scenario, a proton (and its associated charge) is transported from the Y_Z site and, either directly or via intermediate carriers, is released into the bulk medium. Upon reduction of $Y_Z^{\cdot}$, a proton is taken up from the bulk again and transported back to the tyrosine via D1-H190. Figure 2*b* illustrates Y_Z oxidation at a pH below the pK of D1-H190 in the presence of $Y_Z^{\cdot}$. As suggested by Diner *et al.* (1998), at low pH the oxidation may occur as a gated process in which D1-H190(H^+) is first deprotonated by another base in the vicinity and then forms a H-bonding connection to Y_Z. Oxidation occurs once a properly orientated tyrosine/D1-H190 complex is formed. In the model shown in figure 2*b*, the bulk pH is below the pK of D1-H190($Y_Z^{\cdot}$) and, consequently, there is a substoichiometric proton release from the site. Under these conditions, there is a charge associated with the tyrosine site during the lifetime of the radical.

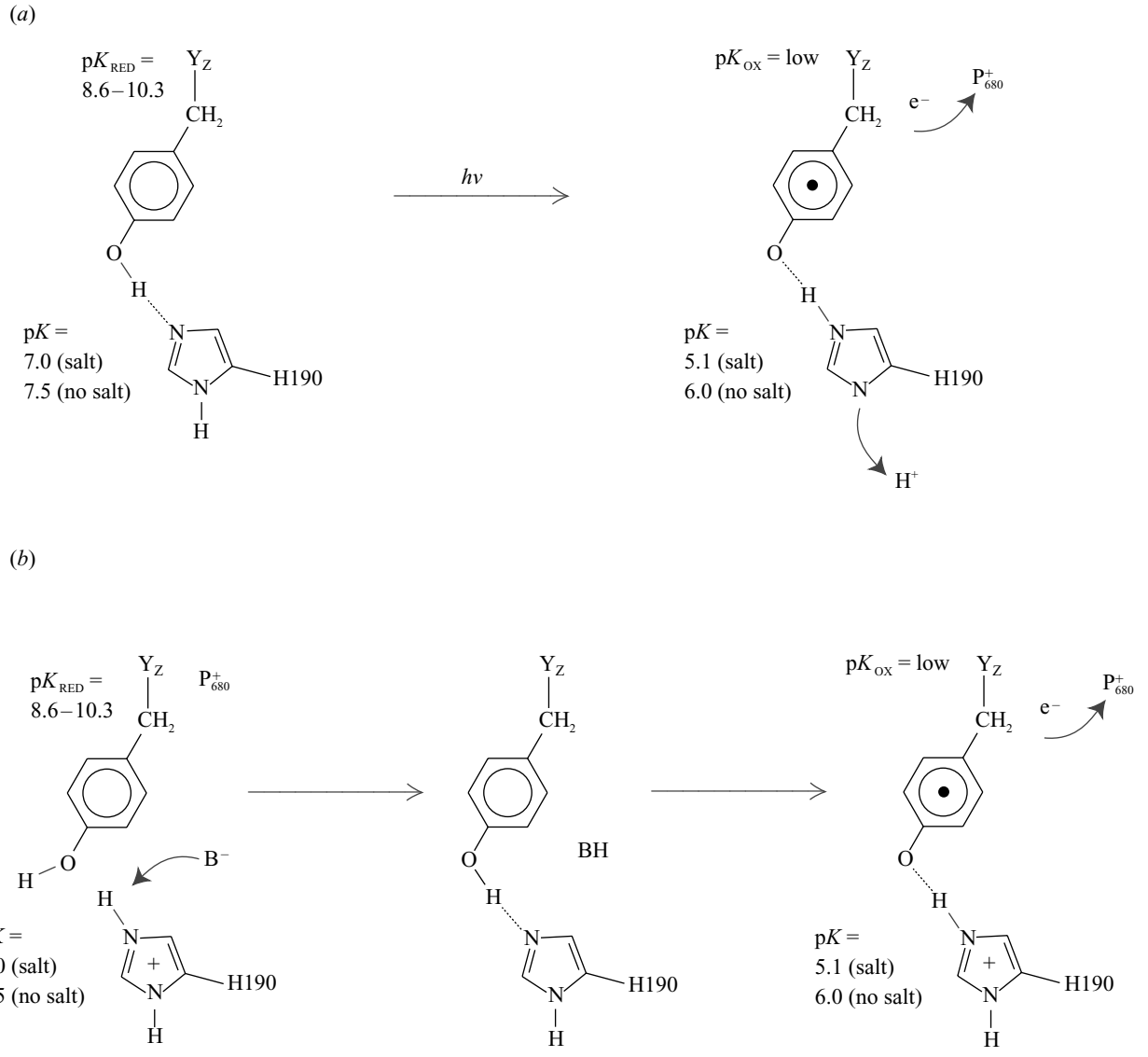

Figure 2. Proton-transfer reactions associated with the oxidation of Y_Z in apo-PSII. The assignments of the pK values are described in § 4. (*a*) Oxidation of Y_Z at pH values above the pK of the H-bonding partner to reduced Y_Z. (*b*) Oxidation of Y_Z at pH values below the pK of the H-bonding partner to oxidized Y_Z.

5. OXIDATION OF Y_Z IN APO-PSII

The reduction of P^+_{680} displays multiphasic kinetics in apo-PSII, as described in § 4. The dominating kinetic components represent the oxidation of Y_Z and the back reaction from Q_A^-. The kinetic components assigned to Y_Z oxidation are pH-dependent and display kinetic deuterium isotope effects. The $Y_Z \rightarrow P^+_{680}$ electron-transfer reaction occurs with half-times spanning from *ca.* 250 ns to 40 μs (Ahlbrink *et al.* 1998; Hays *et al.* 1999). The amplitudes of the sub-microsecond to microsecond kinetic components dominate at high pH. The H/D isotope effects are small in the alkaline pH range and decrease to less than 1.1 at pH 9.0 in PSII cores from pea (Ahlbrink *et al.* 1998). In *Synechocystis* samples, the deuterium isotope effects decrease to 1.1 at pH 9.5 according to Diner *et al.* (1998), or to 1.7 at pH 10.0 according to Hays *et al.* (1999). The rapid kinetic phases have been assigned to Y_Z in favourable H-bonding geometries with D1-H190, as described in § 4 and shown in figure 2*a*. The microsecond, to tens of microsecond, kinetic components dominate at acid pH. The H/D isotope effects increase to *ca.* 2.5 and the activation energy for the $Y_Z \rightarrow P^+_{680}$ electron-transfer reaction increases from 150 meV at pH 8.0 to 300 meV at pH 5.0 (Ahlbrink *et al.* 1998; Hays *et al.* 1999). These characteristics are consistent with the gated oxidation model shown in figure 2*b*.

Different oxidation mechanisms for Y_Z have been discussed in detail by several authors (Diner *et al.* 1998; Renger *et al.* 1998; Hays *et al.* 1999; Tommos & Babcock 2000; Debus 2001; Diner 2001). Briefly, the oxidation of Y_Z to Y_Z could occur according to three main mechanisms: (i) rapid proton transfer followed by rate-limiting electron tunnelling; (ii) rate-limiting proton transfer followed by electron tunnelling; or (iii) as a concerted electron/proton-transfer event. A weak correlation between the oxidation rate and the driving force (Diner *et al.* 1998) and the pH characteristics of Y_Z oxidation (Hays *et al.* 1999) are not consistent with the first mechanism. The two latter reactions cannot be distinguished based on data obtained on apo-PSII, thus far. It is also possible that

the overall oxidation process involves a mixture of events. At low pH, for example, protonic rate limitations are involved in the formation of an H-bonding link between Y_Z and the neutral D1-H190. Once the H-bonded complex is formed, oxidation proceeds via a concerted mechanism. Styring, Hammarström and their co-workers have recently reported an interesting study on the oxidation of tyrosine in water (Sjödin *et al.* 2000). The tyrosine was attached covalently to a ruthenium complex, which served as the light-induced oxidant. At a pH below pK_{RED} of the tyrosine, the rate of oxidation increased with pH from a $t_{1/2}$ of 170 μs at pH 5.0 to 5 μs at pH 9.0. Above pH 10, the rate increased in a stepwise fashion to *ca*. 15 ns and became pH-independent. At pH 10, the oxidation event displayed biphasic kinetics with a mixture of the slow pH-dependent and the fast pH-independent component. In the ruthenium system, the oxidation of the tyrosine occurs as a concerted proton/electron-transfer reaction and the authors proposed a similar oxidation mechanism for Y_Z in apo-PSII (Sjödin *et al.* 2000).

A number of apo-PSII data suggest that Y_Z resides in a solvent-exposed disordered environment and these properties are expected to increase reorganization and activation energies that, in turn, will decrease the electron-transfer rate relative to that of the active enzyme (Tommos & Babcock 2000). Electron magnetic resonance data on $Y_Z^{\cdot}$ show heterogeneity in the position of the phenolic head group and disordered H-bonding (Force *et al.* 1995; Tommos *et al.* 1995; Un *et al.* 1996). Fourier transform infrared spectra of $Y_Z^{\cdot}/Y_Z$ indicate disorder also in the H-bonding of reduced Y_Z (Berthomieu *et al.* 1998). It appears likely that the tyrosine in both of its redox states has multiple H-bonding partners that may include water, other side chains, D1-H190 or D1-H190(H^+). The exact H-bonding geometry will depend on sample conditions, including organism, pH, salt concentration and potentially the temperature. Berthomieu *et al.* (1998) reported that the $Y_Z^{\cdot}/Y_Z$ FTIR spectrum suggests that Y_Z, in its reduced state, is H-bonded to a neutral histidine. The authors also noted that in a minority of PSII centres, the H-bonding partner could be water, a hydroxylated side chain or a protonated histidine. The FTIR study was done under conditions in which the majority of D1-H190 is predicted to be protonated according to the kinetic work described in § 4 and in the text above. We hope that a pH study of the $Y_Z^{\cdot}/Y_Z$ FTIR spectrum could clarify this issue. For the oxidized state, it is possible that the strength of the proposed $Y_Z^{\cdot}$/D1-H190 H-bond varies as a function of pH. A density functional theory investigation on a H-bonded phenol–imidazole complex in gas phase reports an oxygen–nitrogen distance of 2.64 Å for a protonated imidazolium and 2.92 Å for a deprotonated imidazole (O'Malley 1998). Alternatively, the H-bonding contact between D1-H190 and the radical is indirect or broken, as suggested by EMR data (R. D. Britt, personal communication). In apo-PSII, the tyrosine is in facile contact with the bulk medium. This has been shown by EMR studies and by the rapid accessibility of external reductants and small organic bases to the site (see Debus 2001; Tommos & Babcock 2000). Accessibility is necessary for the light-dependent assembly of the catalytic centre, which requires the entry of Mn^{2+} and Ca^{2+} ions to the site (Ananyev *et al.* 2001).

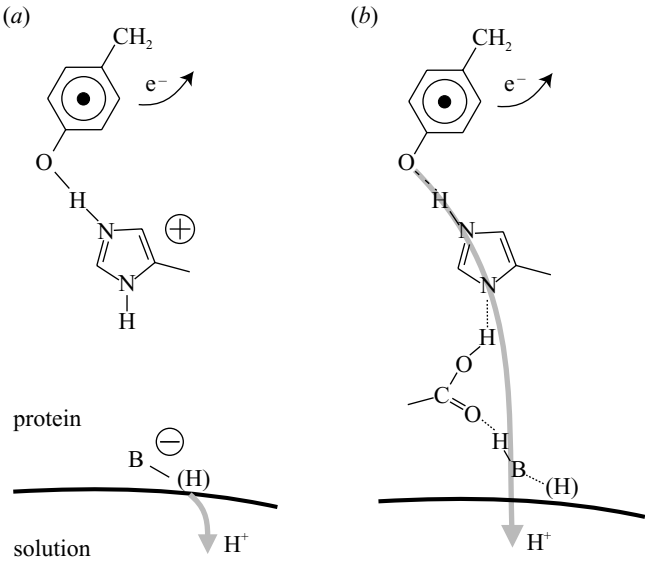

Figure 3. Mechanistic models to describe the light-induced proton release from the donor side of PSII. (*a*) Proton release according to a Bohr mechanism in which electrostatic effects give rise to the proton release. (*b*) Domino-deprotonation release from the tyrosine via a hydrogen-bonded chain or web.

These data strongly suggest that the Y_Z site is in protonic contact with the bulk medium in apo-PSII.

6. EXTENT OF LIGHT-INDUCED PROTON RELEASE FROM APO-PSII

The oxidation model of Y_Z described in figure 2 predicts that the pH and salt concentration in the buffer will modulate the extent of proton release from the Y_Z site upon light excitation. At the alkaline limit, the proton-release stoichiometry will be determined by the pK_{RED} of Y_Z and at the acid limit by the pK of the acceptor for the phenolic proton in the presence of $Y_Z^{\cdot}$. The proton release will also reflect the overall amount of Y_Z that is oxidized. A decrease in radical formation occurs at acid pH, as shown by a steep increase in the Q_A^-/P_{680}^+ back reaction. The extent of proton release from apo-PSII as a function of pH is described below and shown to correlate well with these predictions.

Upon light excitation of apo-PSII, protons are rapidly released from the donor side. The low-pH pulse observed in the bulk medium is reversed upon the reduction of $Y_Z^{\cdot}$. The total extent of released protons can be estimated since the release rate (tens to hundreds of microseconds) is fast relative to the rate of proton rebinding (tens of milliseconds). Two different mechanisms have been proposed to explain the observed proton release/uptake associated with the Y_Z redox cycle. These are illustrated schematically in figure 3. Figure 3*a* pictures a Bohr mechanism in which the proton release to the bulk medium is driven by electrostatic effects. Figure 3*b* describes a domino-release mechanism in which a net proton transport from Y_Z to the bulk phase occurs.

In an early study, Renger & Voelker (1982) studied light-induced proton release from the donor side of PSII in inside-out thylakoids at pH 6.5. These authors concluded that the proton-release stoichiometry was pro-

portional to the extent of oxidation of the primary electron donor to P_{680}^+, which was later identified as Y_Z. They observed that release was close to one proton per reaction centre and concluded that the donor has a p*K* greater than or equal to 8 in the dark and less than 5 in its oxidized form. Rappaport & Lavergne (1997) investigated the proton release from PSII cores prepared from *C. reinhardii* using no salt in the buffer. They measured the release of about one proton at pH above 7 and a substoichiometric release at lower pH approaching 0 below pH 5. It was concluded that the p*K* of the proton donor must be greater than or equal to 9 in the dark in order to give rise to the release of one full proton at pH 7.5. They noted that the proton release titrated with the same p*K* of 6.0 as the $Q_A^-/Y_Z^{\cdot}$ back reaction, and suggested that the same base controls both events. Rappaport & Lavergne (1997) interpreted their data according to a Bohr model in which the phenolic proton of Y_Z remains locally trapped upon oxidation and a charge is associated with the $Y_Z^{\cdot}$ site. The charge formed upon oxidation of Y_Z shifts the p*K* of a nearby base from greater than or equal to 9 to 6. Alternatively, within a domino-release model, the proton donor with a p*K* of greater than or equal to 9.0 in the dark is Y_Z. At a pH above 7.0, more than 90% of D1-H190($Y_Z^{\cdot}$) deprotonates upon light absorption and gives rise to the essentially stoichiometric release (figure 2*a*). The proton release titrates at lower pH with the p*K* of D1-H190($Y_Z^{\cdot}$), which is 6.0 in the absence of salt (figure 2*b*). Ahlbrink *et al.* (1998) reported the proton release from pea core particles between a pH of 4.7 and 7. The extent of proton release was close to one above pH 5.5 and then decreased steeply to *ca.* 0.2 H^+ at pH 4.7. The authors explained the release pattern as follows. Above pH 6, the proton released from Y_Z upon oxidation is trapped inside the protein and gives rise to a charge. This charge shifts p*K*s of peripheral groups that deprotonate to the bulk medium. A direct release from Y_Z was proposed to occur only below pH 6. The proton release from the pea samples was measured in the presence of salt. As described in § 4, the p*K* of D1-H190($Y_Z^{\cdot}$) dropped from 6.0 to 5.1 upon $MgCl_2$ addition to membrane samples. Within a domino-deprotonation model, the shift in the proton titration curve towards lower pH in the study by the Junge group relative to the data reported by Rappaport & Lavergne is explained by a salt effect on the p*K* of D1-H190($Y_Z^{\cdot}$). In addition, Ahlbrink *et al.* (1998) showed that the Q_A^-/P_{680}^+ back reaction increases rapidly below pH 6 and reaches a total extent of *ca*. 60% at pH 4.0. In centres in which 60% of P_{680}^+ is reduced via a back reaction with Q_A^-, a maximum of 0.4 $Y_Z^{\cdot}$ is formed. Thus, the observed rapid decrease in the proton release at acid pH also reflects a decrease in the formation of $Y_Z^{\cdot}$. In conclusion, a domino-deprotonation mechanism can accurately describe the extent of light-induced proton release from apo-PSII reported in the literature. Arguments against domino deprotonation of Y_Z to the bulk medium have been based on the assumption that the lower p*K* for the proton-release data should reflect the pK_{OX} of Y_Z (Rappaport & Lavergne 1997; Diner 2001). In contrast, it is argued here that the low p*K* for the proton-release stoichiometry is determined by the p*K* of the H-bonding partner to $Y_Z^{\cdot}$ and by the pH-dependence of $Y_Z^{\cdot}$ formation.

The situation described above pertains to apo-PSII but is likely to change dramatically in holo-PSII, in which the functional metal cluster is assembled and the active site is protected by a *ca*. 40 Å layer of protein matrix represented by the extrinsic proteins (Zouni *et al.* 2001: Nield *et al.* 2002). The characteristics of Y_Z oxidation in O_2-evolving samples are discussed in the following sections.

7. THE PROTONATION STATE OF Y_Z IN HOLO-PSII

Fourier transform infrared data suggest that Y_Z is protonated at physiological pH in active (Noguchi *et al.* 1997) and calcium-depleted (Berthomieu *et al.* 1998; Diner 2001) PSII samples. In addition, deuterium kinetic isotope effects show that there are protonic reactions coupled to the oxidation of Y_Z in holo-PSII (see § 8 below). Finally, the reduction potential of Y_Z is consistent with the potential of a neutral $Y^{\cdot}/Y$ redox pair (Tommos & Babcock 2000). The CW-EPR spectrum representing oxidized Y_Z in O_2-evolving PSII has the same line shape as the spectra of $Y_D^{\cdot}$ in active centres and $Y_Z^{\cdot}$ in apo-PSII (Hoganson & Babcock 1988). These observations show that Y_Z forms a neutral radical in holo-PSII since the spin-density distribution of a tyrosine cation radical differs substantially from that of a neutral radical (Box *et al.* 1974). In conclusion, Y_Z is protonated at physiological pH and is oxidized to a deprotonated radical. D1-H190 is believed to serve as a proton acceptor upon oxidation of Y_Z in active PSII. This conclusion is based on analogies to Y_D and D2-H189 (see § 3 above), the kinetics of Y_Z oxidation in D1-H190 mutants (Debus 2001) and FTIR data (Diner 2001). Although a wealth of data suggest that the tyrosine and histidine are functionally coupled, the exact geometry remains to be established. D1-E189 may also be involved in proton-transfer reactions upon Y_Z oxidation (Clausen *et al.* 2001).

8. Y_Z OXIDATION IN HOLO-PSII

The $Y_Z \rightarrow P_{680}^+$ electron-transfer reaction is also multiphasic in the active enzyme, but the rates, the pH-dependence, the deuterium kinetic isotope effects and the activation energies differ substantially as compared with apo-PSII. Approximately 80–85% of Y_Z is oxidized on the nanosecond time-scale with biphasic kinetics that is moderately faster in the lower S-states. The remaining 15–20% of Y_Z is oxidized on the tens of microseconds time-scale (Rappaport & Lavergne 2001; Renger 2001; Jeans *et al.* 2002). The nanosecond kinetic phases of Y_Z oxidation are insensitive to H_2O/D_2O exchange. By contrast, the microsecond kinetic components exhibit a significant H/D isotope effect (Schilstra *et al.* 1998; Christen *et al.* 1999). Witt and co-workers studied the $Y_Z \rightarrow P_{680}^+$ reaction in *Synechococcus* and noted that the rate was S-state-dependent and weakly dependent on the pH (Meyer *et al.* 1989). In S_0 and S_1, the majority of P_{680}^+ was reduced with a $t_{1/2}$ of 40 ns at pH 4.0, which decreased to 20 ns at pH 7.0. In S_2 and S_3, the reduction rate was biphasic at neutral pH with $t_{1/2}$ = 40/280 ns. The amplitude of the slower kinetic component became dominant at acid pH. Christen *et al.* (1999) studied the relative amplitudes of the nanosecond kinetic components as a function of pH in spinach thylakoids. The amplitudes decrease rapidly below pH

6.5, which was suggested to arise from either protonation of the H-bonding partner to Y_Z or from acid-induced calcium release. The early work by the Witt group is in agreement with a recent study, with the exception that biphasic kinetics was reported for P_{680}^+ reduction in the nanosecond time-scale in all S-states. Klug and co-workers studied the decay of P_{680}^+ between 5 and 25 °C in PSII-enriched membranes at pH 6.5 (Jeans *et al.* 2002). At 15 °C, the fastest phase of P_{680}^+ decay was *ca.* 50 ns in the lower S-states and 90 ns in the higher S-states. The slower component in the biphasic kinetics was *ca.* 500 ns in S_0 and S_1 and 700 ns in S_2 and S_3. The free energy for the $Y_Z \rightarrow P_{680}^+$ reaction is time-dependent (Jeans *et al.* 2002). Approximately 2 μs after light excitation, ΔG was estimated at *ca.* –40 meV in S_0 and S_1 and –30 meV in S_2 and S_3. On the microsecond time-scale, the driving force increased further by –20 meV in all S-states. Changes in ΔG as a function of temperature and across the S-states were small, typically 10 mV or less. By contrast, the activation energy of Y_Z oxidation differs substantially between the lower and higher S-states. Jeans *et al.* (2002) reported an activation energy of *ca.* 50 meV for the nanosecond kinetic components in S_0 and S_1 that increases to *ca.* 260 meV in the higher S-states. The activation energy was estimated at *ca.* 250 meV for the microsecond kinetics in all S-states. Jeans *et al.* (2002) suggested that the increase in activation energy in the higher S-states could arise from charge accumulation at the manganese cluster in the $S_1 \rightarrow S_2$ transition. As described above, the free energy for the $Y_Z \rightarrow P_{680}^+$ reaction is essentially S-state-independent. This observation would argue against charge accumulation.

Based on the high potential of the $Y^{\cdot+}/Y$ redox pair, it is unlikely that oxidation of Y_Z in holo-PSII occurs via a transient tyrosine cation radical (Tommos & Babcock 2000). The absence of kinetic H/D effects suggests that rate-limiting proton transfer followed by electron tunnelling does not occur either. Thus, oxidation of Y_Z on the nanosecond time-scale may occur by rapid proton transfer followed by rate-limiting electron tunnelling, or as a concerted electron/proton-transfer event. The nanosecond oxidation rate of Y_Z has been compared with calculated electron-tunnelling rates (Renger *et al.* 1998; Tommos & Babcock 2000; Jeans *et al.* 2002) using the relationship derived by Dutton, Moser and co-workers (Page *et al.* 1999). The oxidation of Y_Z is a proton-coupled event and these estimations may not describe the situation accurately but, nonetheless, they illustrate that the oxidation of Y_Z is remarkably fast in O_2-evolving PSII. The slow oxidation rate observed for tyrosine in water (Sjödin *et al.* 2000) also supports this conclusion. The picture that emerges is that of a site well designed for efficient electron and proton transfer. This is consistent with the function of Y_Z to secure a high quantum yield for the charge-separating event. The characteristics of the $Y_Z \rightarrow P_{680}^+$ electron-transfer reaction suggest proton migration from the tyrosine site to complete the reduction (Tommos & Babcock 2000; Rappaport & Lavergne 2001; Renger 2001). The multiphasic oxidation event could be explained by a homogeneous or heterogeneous relaxation mechanism. With the latter model, the multiphasic oxidation rate is described as follows. Oxidation of the tyrosine triggers a domino-deprotonation through an H-bonding network to some final acceptor(s). At the instant of the flash, the geometry of this network differs between PSII centres. The slower kinetic components represent centres in which reorganization of the proton-transfer network must occur to complete the reduction of P_{680}^+. A second question with respect to the proton transfer induced by Y_Z oxidation is how far the proton moves. Is it just a local event (Rappaport & Lavergne 2001) or does it involve more extended H-bonding networks (Tommos & Babcock 2000; Renger 2001)? Is the proton-transfer pathway isolated in the protein matrix or in equilibrium with the bulk phase? The function of Y_Z described in figure 1 requires the latter to occur. As noted earlier, time-resolved measurements on proton release from the donor side of PSII upon light excitation show rapid release in all S-state transitions (Haumann & Junge 1994). The measurements using indicator dyes have a maximum time-resolution of *ca.* 10 μs and, under such conditions, no saturation of the proton-release rate was observed in unstacked thylakoids (Haumann & Junge 1994) or PSII core samples (Bögershausen & Junge 1995). These observations are consistent with a domino-deprotonation from Y_Z to the bulk phase.

The interpretation of the dye measurements varies between groups. Junge and co-workers explain the rapid proton release as electrostatic events in both native samples (Haumann & Junge 1994; Bögershausen & Junge 1995) and for apo-PSII above pH 6.0 (Ahlbrink *et al.* 1998). Rappaport & Lavergne (2001) have suggested that the dye could diffuse to the tyrosine site and monitor internal proton release. This argument was based on the chemical rescue experiments on manganese-depleted wild-type and D1-H190 mutants by Debus and co-workers (Hays *et al.* (1999) and references therein). That the dye could come close to Y_Z in apo-PSII appears reasonable considering the accessibility of the tyrosine site. Access by the dye to the tyrosine site in holo-PSII is less likely since the characteristics of the site are very different in O_2-evolving samples as compared with apo-PSII. A domino-deprotonation model fits well with the extent of proton release over the whole pH range in apo-PSII (see § 6 above). At higher pH in the Mn-depleted system, the rate of electron transfer is faster than proton transfer, as monitored by pH-sensitive dyes. The rates of Y_Z oxidation and proton release were similar below pH 6 and this was interpreted by Ahlbrink *et al.* (1998) to indicate that only under these conditions does chemical release from the tyrosine to the bulk occur. This observation may be an effect of the dye since only at low pH is the oxidation rate of Y_Z slow enough (tens of microseconds) to occur on the same time-scale as the time-resolution of the indicator dye measurements.

9. EXTENT OF PROTON RELEASE FROM ACTIVE PSII

The patterns of proton release from the donor side of O_2-evolving PSII samples can be divided into two main classes. PSII preparations that belong to the first class give rise to non-stoichiometric, S-state and pH-dependent proton release. By contrast, the second class of PSII samples exhibits integer and pH-independent proton release for each transition in the catalytic cycle. S-state and pH-dependent proton release have been observed in three dif-

ferent sample preparations. These include unstacked thylakoid membranes from pea (Haumann & Junge 1994), which contain the complete set of PSII proteins including LHCII, CP24, CP26 and CP29 as well as the extrinsic 33, 23 and 17 kDa proteins. The second preparation with non-stoichiometric release is PSII-enriched membranes from spinach (Rappaport & Lavergne 1991). These samples also contain the complete PSII complex including the outer antenna and the extrinsic proteins. Recently, Schlodder & Witt (1999) reported a non-integer release from PSII core samples prepared from thermophilic *S. elongatus*. These core samples contain the 33 kDa, 15 kDa (cyt. c_{550}) and 12 kDa proteins that are the equivalents to the extrinsic proteins of higher plants. The stoichiometric, pH-independent 1 : 1 : 1 : 1 proton release pattern is observed in various PSII core preparations from pea, spinach and *Synechocystis* (Lübbers *et al.* 1993; Haumann *et al.* 1997). PSII cores are not membrane samples and the higher plant preparations do not contain LHCII. In addition, in some core samples one or several of the extrinsic proteins are absent (Haumann *et al.* 1997). A non-oscillating release has also been observed from modified membrane preparations. Thylakoids grown in intermittent light give rise to no, or very weak, oscillations in the proton-release pattern (Lavergne & Junge 1993; Haumann *et al.* 1997). The light treatment impairs chlorophyll *b* synthesis and these samples do not contain LHCII, CP24 or CP29 (Lavergne & Junge 1993; Haumann *et al.* 1997). A short incubation at a low concentration of detergent abolishes the non-integer proton-release pattern in PSII-enriched membrane samples. The detergent treatment solubilizes LHCII and the 17 and 23 kDa extrinsic proteins (Haumann *et al.* 1997).

The pattern of proton release over the S-state cycle varies significantly between the three preparations of the first class. In the $S_1 \rightarrow S_2$ transition, for example, less than 0.1 H^+ is released from PSII-enriched membranes at pH 6.0 (Rappaport & Lavergne 1991). From thylakoid samples, however, more than 1.5 protons are released at pH 6.0 in the same transition (Haumann & Junge 1994). Nonetheless, there are trends in the data, including the following. The total release varies between 0 and 2 H^+ at all pH values studied. The proton release is generally less in the $S_1 \rightarrow S_2$ transition relative to the $S_0 \rightarrow S_1$ and $S_3 \rightarrow S_0$ transitions. A stoichiometric proton release is always observed in the $S_2 \rightarrow S_3$ transition, independent of material and pH. The variability in the proton release appears to correlate with the intactness of the PSII sample (see fig. 2 in Lavergne & Junge 1993). The changes in the proton release as a function of pH are most pronounced in intact thylakoids. The release pattern is smoother in PSII-enriched membranes and eventually becomes stoichiometric and pH-independent in the modified preparations.

The characteristics of the proton release from the various samples described above suggest that the release of substrate protons is distributed over the catalytic cycle. In addition, the pH-dependence of the proton release indicates the existence of Bohr effects in the more intact samples. Based on these considerations, the observed proton release for any S-state transition can be described as follows, where x and y indicate the amount of chemical and Bohr protons, respectively:

$S_n \rightarrow S_{n+1}$: observed H^+ (observed) = $x H^+$ (chemical) $\pm y H^+$ (Bohr).

The observed proton-release pattern contains contributions from chemical protons, which are defined here as protons release from the $(Mn)_4/Y_Z$ site. The chemical protons may be released either from the manganese cluster or from Y_Z. The observed release also reflects proton release or uptake that are driven by Bohr effects. Bohr protons are released or bound by amino acids that change their p*K*s in response to an electrostatic or structural change. Both the chemical and the Bohr protons are expected to be sensitive to the dielectric constant of the protein medium. Nonetheless, it is reasonable to assume that the Bohr protons are more sensitive to the average dielectric constant of the protein as compared with the chemical protons. Bohr effects are directly related to the average dielectric constant of the protein medium and will decrease as the dielectric constant of the medium increases. Consequently, the contribution from the chemical protons should become more pronounced in samples in which the average dielectric constant is high. A persistent theme with the proton-release data is that in more biochemically resolved samples, the stoichiometric and pH-independent release pattern emerges. In the dielectric-dependent model for the proton release presented here, this 1 : 1 : 1 : 1 pattern represents substrate protons that are released either directly from the manganese cluster or via the tyrosine.

As described earlier, the H-atom abstraction model predicts the release of one substrate proton per S-state transition. The model is overall charge-neutral, but it does not exclude the formation or collapse of dipoles during the catalytic cycle, which in turn could give rise to the observed Bohr effects. The inorganic part of the active site contains four manganese ions, calcium and chloride. Changes in oxidation states and potential ligand rearrangements associated with the catalytic cycle are likely to introduce dipoles in the active site. This could occur by oxidizing one manganese ion in the cluster while deprotonation occurs at a second manganese ion. Another possible source for Bohr effects is movement of the chloride anion. Chloride has been proposed to ligate to the metal cluster in $S_1 \rightarrow S_2$ and be released again in $S_3 \rightarrow S_0$ on the basis of Jahn–Teller effects (Tommos & Babcock 1998). An observation consistent with this suggestion is that the extent of proton release in the $S_1 \rightarrow S_2$ transition is stoichiometric and pH-independent in Cl^--depleted thylakoids (Haumann *et al.* 1996).

10. CONCLUDING REMARKS

A proton-coupled electron-transfer function for Y_Z in photosynthetic water oxidation was proposed seven years ago (Babcock 1995; Hoganson *et al.* 1995; Tommos *et al.* 1995). This function for Y_Z has been incorporated into several mechanistic models for the catalytic cycle of PSII, although the extent of Y_Z involvement in substrate proton delivery from the active site to the thylakoid lumen in different S-state transitions remains controversial. A key mechanistic step in the proposed function for Y_Z is proton transfer from the tyrosine site upon oxidation. This paper described oxidation mechanisms for Y_Z in apo-PSII and

in the active enzyme. A domino-deprotonation model from the tyrosine to the bulk solution was shown to be consistent with a variety of data obtained on the apo system. Experimental data that suggest that the oxidation of Y_Z in O_2-evolving samples is coupled to proton transfer in an H-bonding network were described. A direct link between the redox-driven proton transfers within the protein and proton release into the bulk solution remains, however, to be proven. Finally, a dielectric-dependent model was proposed to rationalize the variability in the proton release associated with the catalytic cycle as a function of sample preparation.

The author thanks Anders Ehrenberg, Per Siegbahn, Margareta Blomberg and the research groups of Peter Brzezinski, Stenbjörn Styring and Mårten Wikström for valuable discussions. Financial support by the Swedish Research Council is gratefully acknowledged. This paper is dedicated to the memory of Jerry Babcock.

REFERENCES

Ahlbrink, R., Haumann, M., Cherepanov, D., Bögershausen, O., Mulkidjanian, A. & Junge, W. 1998 Function of tyrosine Z in water oxidation by photosystem II: electrostatical promotor instead of hydrogen abstractor. *Biochemistry* **37**, 1131–1142.

Ananyev, G. M., Zaltsman, L., Vasko, C. & Dismukes, G. C. 2001 The inorganic biochemistry of photosynthetic oxygen evolution/water oxidation. *Biochim. Biophys. Acta* **1503**, 52–68.

Ananyev, G. M., Sakiyan, I., Diner, B. A. & Dismukes, G. C. 2002 A functional role for tyrosine-D in assembly of the inorganic core of the water oxidise complex of photosystem II and the kinetics of water oxidation. *Biochemistry* **41**, 974–980.

Babcock, G. T. 1995 The oxygen-evolving complex in photosystem II as a metallo-radical enzyme. In *Photosynthesis: from light to biospere*, vol. II (ed. P. Mathis), pp. 209–215. Dordrecht, The Netherlands: Kluwer.

Babcock, G. T., Barry, B. A., Debus, R. J., Hoganson, C. W., Atamian, M., McIntosh, L., Sithole, I. & Yocum, C. F. 1989 Water oxidation in photosystem II: from radical chemistry to multielectron chemistry. *Biochemistry* **28**, 9557–9565.

Berthomieu, C., Hienerwadel, R., Boussac, A., Breton, J. & Diner, B. A. 1998 Hydrogen bonding of redox-active tyrosine Z of photosystem II probed by FTIR difference spectroscopy. *Biochemistry* **37**, 10 547–10 554.

Bögershausen, O. & Junge, W. 1995 Rapid proton transfer under flashing light in both functional sides of dark-adapted photosystem II particles. *Biochim. Biophys. Acta* **1230**, 177–185.

Bordwell, F. G. & Cheng, J.-P. 1991 Substituent effects on the stabilities of phenoxyl radicals and the acidities of phenoxyl radical cations. *J. Am. Chem. Soc.* **113**, 1736–1743.

Box, H. C., Budzinski, E. E. & Freund, H. G. 1974 Effects of ionizing radiation on tyrosine. *J. Chem. Phys.* **61**, 2222–2226.

Campbell, K. A., Peloquin, J. M., Diner, B. A., Tang, X.-S., Chisholm, D. A. & Britt, R. D. 1997 The τ-nitrogen of D2 histidine 189 is the hydrogen bond donor to the tyrosine radical $Y_D^{\cdot}$ of photosystem II. *J. Am. Chem. Soc.* **119**, 4787–4788.

Carrell, T. G., Tyryshkin, A. M. & Dismukes, G. C. 2002 An evaluation of structural models for the photosynthetic water-oxidizing complex derived from spectroscopic and X-ray diffraction signatures. *J. Biol. Inorg. Chem.* **7**, 2–22.

Christen, G., Seeliger, A. & Renger, G. 1999 $P680^{+\cdot}$ reduction kinetics and redox transition probability of the water oxidizing complex as a function of pH and H/D isotope exchange in spinach thylakoids. *Biochemistry* **38**, 6082–6092.

Clausen, J., Winkler, S., Hays, A.-M. A., Hundelt, M., Debus, R. J. & Junge, W. 2001 Photosynthetic water oxidation in *Synechocystis* sp. PCC6803: mutations D1-E189K, R and Q are without influence on electron transfer at the donor side of photosystem II. *Biochim. Biophys. Acta* **1506**, 224–235.

Conjeaud, H. & Mathis, P. 1980 The effect of pH on the reduction kinetics of P-680 in tris-treated chloroplasts. *Biochim. Biophys. Acta* **590**, 353–359.

Dau, H., Iuzzolino, L. & Dittmer, J. 2001 The tetra-manganese complex of photosystem II during its redox cycle—X-ray absorption results and mechanistic implications. *Biochim. Biophys. Acta* **1503**, 24–39.

Debus, R. J. 2001 Amino acid residues that modulate the properties of tyrosine Y_Z and the manganese cluster in the water oxidizing complex of photosystem II. *Biochim. Biophys. Acta* **1503**, 164–186.

Diner, B. A. 2001 Amino acid residues involved in the coordination and assembly of the manganese cluster of photosystem II. Proton-coupled electron transport of the redox-active tyrosines and its relationship to water oxidation. *Biochim. Biophys. Acta* **1503**, 147–163.

Diner, B. A., Force, D. A., Randall, D. W. & Britt, R. D. 1998 Hydrogen bonding, solvent exchange, and coupled proton and electron transfer in the oxidation and reduction of redox-active tyrosine Y_Z in Mn-depleted core complexes of photosystem II. *Biochemistry* **37**, 17 931–17 943.

Diner, B. A., Schlodder, E., Nixon, P. J., Coleman, W. J., Rappaport, F., Lavergne, J., Vermaas, W. F. J. & Chisholm, D. A. 2001 Site-directed mutations at D1-His189 and D2-His197 of photosystem II in *Synechocystis* PCC 6803: sites of primary charge separation and cation and triplet stabilization. *Biochemistry* **40**, 9265–9281.

Dixon, W. T. & Murphy, D. 1976 Determination of the acidity constants of some phenol radical cations by means of electron spin resonance. *J. Chem. Soc., Faraday Trans. II* **72**, 1221–1230.

Faller, P., Debus, R. J., Brettel, K., Sugiura, M., Rutherford, A. W. & Boussac, A. 2001 Rapid formation of the stable tyrosyl radical in photosystem II. *Proc. Natl Acad. Sci. USA* **98**, 14 368–14 373.

Force, D. A., Randall, D. W., Britt, R. D., Tang, X.-S. & Diner, B. A. 1995 ^{2}H ESE-ENDOR study of hydrogen bonding to the tyrosine radicals $Y_D^{\cdot}$ and $Y_Z^{\cdot}$ of photosystem II. *J. Am. Chem. Soc.* **117**, 12 643–12 644.

Gilchrist Jr, M. L., Ball, J. A., Randall, D. W. & Britt, R. D. 1995 Proximity of the manganese cluster of photosystem II to the redox-active tyrosine Y_Z. *Proc. Natl Acad. Sci. USA* **92**, 9545–9549.

Haumann, M. & Junge, W. 1994 Extent and rate of proton release by photosynthetic water oxidation in thylakoids: electrostatic relaxation versus chemical production. *Biochemistry* **33**, 864–872.

Haumann, M. & Junge, W. 1999 Photosynthetic water oxidation: a simplex-scheme of its partial reactions. *Biochim. Biophys. Acta* **1411**, 86–91.

Haumann, M., Drevenstedt, W., Hundelt, M. & Junge, W. 1996 Photosystem II of green plants. Oxidation and deprotonation of the same component (histidine?) on $S_1^* \rightarrow S_2^*$ in chloride-depleted centers as on $S_2 \rightarrow S_3$ in controls. *Biochim. Biophys. Acta* **1273**, 237–250.

Haumann, M., Hundelt, M., Jahns, P., Chroni, S., Bögershausen, O., Ghanotakis, D. & Junge, W. 1997 Proton release from water oxidation by photosystem II: similar stoichiometries are stabilized in thylakoids and PSII core particles by glycerol. *FEBS Lett.* **410**, 243–248.

Hays, A.-M. A., Vassiliev, I. R., Golbeck, J. H. & Debus, R. J.

1999 Role of D1-H190 in the proton-coupled oxidation of tyrosine Y_Z in manganese-depleted photosystem II. *Biochemistry* **38**, 11 851–11 865.

Hienerwadel, R., Boussac, A., Breton, J., Diner, B. A. & Berthomieu, C. 1997 Fourier transform infrared difference spectroscopy of photosystem II tyrosine D using site-directed mutagenesis and specific isotope labeling. *Biochemistry* **36**, 14 712–14 723.

Hillier, W. & Wydrzynski, T. 2000 The affinities for the two substrate water binding sites in the O_2 evolving complex of photosystem II vary independently during S-state turnover. *Biochemistry* **39**, 4399–4405.

Hoganson, C. W. & Babcock, G. T. 1988 Electron-transfer events near the reaction center in O_2-evolving photosystem II preparations. *Biochemistry* **27**, 5848–5855.

Hoganson, C. W. & Babcock, G. T. 2000 Mechanistic aspects of the tyrosyl radical–manganese complex in photosynthetic water oxidation. In *Metal ions in biological systems*, vol. 37 (ed. H. Sigel & A. Sigel), pp. 613–656. New York: Marcel Dekker.

Hoganson, C. W., Lydakis-Simantiris, N., Tang, X.-S., Tommos, C., Warncke, K., Babcock, G. T., Diner, B. A., McCracken, J. & Styring, S. 1995 A hydrogen-atom abstraction model for the function of Y_Z in photosynthetic oxygen evolution. *Photosynth. Res.* **46**, 177–184.

Jeans, C., Schilstra, M. J. & Klug, D. R. 2002 The temperature dependence of $P680^+$ reduction in oxygen-evolving photosystem II. *Biochemistry* **41**, 5015–5023.

Lavergne, J. & Junge, W. 1993 Proton release during the redox cycle of the water oxidase. *Photosynth. Res.* **38**, 279–296.

Lübbers, K., Haumann, M. & Junge, W. 1993 Photosynthetic water oxidation under flashing light. Oxygen release, proton release and absorption transients in the near ultraviolet—a comparison between thylakoids and a reaction-center core preparation. *Biochim. Biophys. Acta* **1183**, 210–214.

Mamedov, F., Sayre, R. T. & Styring, S. 1998 Involvement of histidine 190 on the D1 protein in electron/proton transfer reactions on the donor side of photosystem II. *Biochemistry* **37**, 14 245–14 256.

Meyer, B., Schlodder, E., Dekker, J. P. & Witt, H. T. 1989 O_2 evolution and Chl $a_{II}{}^+$ ($P\text{-}680^+$) nanosecond reduction kinetics in single flashes as a function of pH. *Biochim. Biophys. Acta* **974**, 36–43.

Nield, J., Balsera, M., De Las Rivas, J. & Barber, J. 2002 3D cryo-EM study of the extrinsic domains of the oxygen evolving complex of spinach: assignment of the psbO protein. *J. Biol. Chem.* **277**, 15 006–15 012.

Noguchi, T., Inoue, Y. & Tang, X.-S. 1997 Structural coupling between the oxygen-evolving Mn cluster and a tyrosine residue in photosystem II as revealed by Fourier transform infrared spectroscopy. *Biochemistry* **36**, 14 705–14 711.

O'Malley, P. J. 1998 Hybrid density functional studies of the oxidation of phenol-imidazole hydrogen-bonded complexes: a model for tyrosine oxidation in oxygenic photosynthesis. *J. Am. Chem. Soc.* **120**, 11 732–11 737.

Page, C. C., Moser, C. C., Chen, X. & Dutton, P. L. 1999 Natural engineering principles of electron tunnelling in biological oxidation–reduction. *Nature* **402**, 47–52.

Pecoraro, V. L., Baldwin, M. J., Caudle, M. T., Hsieh, W.-Y. & Law, N. A. 1998 A proposal for water oxidation in photosystem II. *Pure Appl. Chem.* **70**, 925–929.

Peloquin, J. M. & Britt, R. D. 2001 EPR/ENDOR characterization of the physical and electronic structure of the OEC Mn cluster. *Biochim. Biophys. Acta* **1503**, 96–111.

Rappaport, F. & Lavergne, J. 1991 Proton release during successive oxidation steps of the photosynthetic water oxidation process: stoichiometries and pH dependence. *Biochemistry* **30**, 10 004–10 012.

Rappaport, F. & Lavergne, J. 1997 Charge recombination and proton transfer in manganese-depleted photosystem II. *Biochemistry* **36**, 15 294–15 302.

Rappaport, F. & Lavergne, J. 2001 Coupling of electron and proton transfer in the photosynthetic water oxidase. *Biochim. Biophys. Acta* **1503**, 246–259.

Renger, G. 2001 Photosynthetic water oxidation to molecular oxygen: apparatus and mechanism. *Biochim. Biophys. Acta* **1503**, 210–228.

Renger, G. & Voelker, M. 1982 Studies on the proton release pattern of the donor side of system II: correlation between oxidation and deprotonation of donor D_1 in tris-washed inside-out thylakoids. *FEBS Lett.* **149**, 203–207.

Renger, G., Christen, G., Karge, M., Eckert, H.-J. & Irrgang, K.-D. 1998 Application of the Marcus theory for analysis of the temperature dependence of the reactions leading to photosynthetic water oxidation: results and implication. *J. Biol. Inorg. Chem.* **3**, 360–366.

Rigby, S. E. J., Maclachlan, D. J., Nugent, J. H. A. & O'Malley, P. J. 1994*a* An ENDOR study of structural changes in the environment of the dark stable tyrosine radical, $Y_D^{\cdot}$, of photosystem 2 induced by inhibition of the oxygen evolving complex. *Biochim. Biophys. Acta* **1188**, 318–324.

Rigby, S. E. J., Nugent, J. H. A. & O'Malley, P. J. 1994*b* The dark stable tyrosine radical of photosystem 2 studied in three species using ENDOR and EPR spectroscopies. *Biochemistry* **33**, 1734–1742.

Robblee, J. H., Cinco, R. M. & Yachandra, V. K. 2001 X-ray spectroscopy-based structure of the Mn cluster and mechanism of photosynthetic oxygen evolution. *Biochim. Biophys. Acta* **1503**, 7–23.

Schilstra, M. J., Rappaport, F., Nugent, J. H. A., Barnett, C. J. & Klug, D. R. 1998 Proton/hydrogen transfer affects the S-state-dependent microsecond phases of P680+ reduction during water splitting. *Biochemistry* **37**, 3974–3981.

Schlodder, E. & Witt, H. T. 1999 Stoichiometry of proton release from the catalytic center in photosynthetic water oxidation. *J. Biol. Chem.* **274**, 30 387–30 392.

Siegbahn, P. E. M. 2000 Theoretical models for the oxygen radical mechanism of water oxidation and of the water oxidizing complex of photosystem II. *Inorg. Chem.* **39**, 2923–2935.

Sjödin, M., Styring, S., Åkermark, B., Sun, L. & Hammarström, L. 2000 Proton-coupled electron transfer from tyrosine in a tyrosine–ruthenium–tris-bipyridine complex: comparison with tyrosine_Z oxidation in photosystem II. *J. Am. Chem. Soc.* **122**, 3932–3936.

Tommos, C. & Babcock, G. T. 1998 Oxygen production in nature: a light-driven metalloradical enzyme process. *Acc. Chem. Res.* **31**, 18–25.

Tommos, C. & Babcock, G. T. 2000 Proton and hydrogen currents in photosynthetic water oxidation. *Biochim. Biophys. Acta* **1458**, 199–219.

Tommos, C., Tang, X.-S., Warncke, K., Hoganson, C. W., Styring, S., McCracken, J., Diner, B. A. & Babcock, G. T. 1995 Spin-density distribution, conformation, and hydrogen bonding of the redox-active tyrosine Y_Z in photosystem II from multiple electron magnetic-resonance spectroscopies: implication for photosynthetic oxygen evolution. *J. Am. Chem. Soc.* **117**, 10 325–10 335.

Tommos, C., Hoganson, C. W., Di Valentin, M., Lydakis-Simantiris, N., Dorlet, P., Westphal, K., Chu, H.-A., McCracken, J. & Babcock, G. T. 1998*a* Manganese and tyrosyl radical function in photosynthetic oxygen evolution. *Curr. Opin. Chem. Biol.* **2**, 244–252.

Tommos, C., McCracken, J., Styring, S. & Babcock, G. T. 1998*b* Stepwise disintegration of the photosynthetic oxygen-evolving complex. *J. Am. Chem. Soc.* **120**, 10 441–10 452.

Tommos, C., Skalicky, J. J., Pilloud, D. L., Wand, A. J. & Dut-

ton, P. L. 1999 *De novo* proteins as models of radical enzymes. *Biochemistry* **38**, 9495–9507.
Un, S., Tang, X.-S. & Diner, B. A. 1996 245 GHz high-field EPR study of tyrosine-$D^{\cdot}$ and tyrosine-$Z^{\cdot}$ in mutants of photosystem II. *Biochemistry* **35**, 679–684.
Vass, I. & Styring, S. 1991 pH-dependent charge equilibria between tyrosine-D and the S states in photosystem II. Estimation of relative midpoint redox potentials. *Biochemistry* **30**, 830–839.
Vrettos, J. S., Limburg, J. & Brudvig, G. W. 2001 Mechanism of photosynthetic water oxidation: combinding biophysical studies of photosystem II with inorganic model chemistry. *Biochim. Biophys. Acta* **1503**, 229–245.
Warncke, K., Babcock, G. T. & McCracken, J. 1994 Structure of the Y_D tyrosine radical in photosystem II as revealed by ^{2}H electron spin echo envelope modulation (ESEEM) spectroscopic analysis of hydrogen hyperfine interactions. *J. Am. Chem. Soc.* **116**, 7332–7340.
Wincencjusz, H., van Gorkom, H. J. & Yocum, C. F. 1997 The photosynthetic oxygen evolving complex requires chloride for its redox state $S_2 \rightarrow S_3$ and $S_3 \rightarrow S_0$ transitions but not for the $S_0 \rightarrow S_1$ or $S_1 \rightarrow S_2$ transitions. *Biochemistry* **36**, 3663–3670.
Zouni, A., Witt, H. T., Kern, J., Fromme, P., Krauß, H., Saenger, W. & Orth, P. 2001 Crystal structure of photosystem II from *Synechococcus elongatus* at 3.8 Å resolution. *Nature* **409**, 739–743.

Discussion

L. Sun (*Department of Organic Chemistry, Stockholm University, Stockholm, Sweden*). How is the H-bonding network between Y_Z and His190 re-established after Y_Z has been regenerated from its radical state?

C. Tommos. The residues that participate in the proton transfer from the tyrosine site to the bulk phase must flip in order to reset the pathway for the next oxidation/proton-transfer event. It is possible that the multiphasic characteristics of P^+_{680} reduction reflect the resetting of the proton-transfer pathway. The H/D-isotope-sensitive microsecond kinetic components of P^+_{680} reduction may represent centres in which reorganization of the proton-transfer network must occur to complete the electron transfer between Y_Z and P^+_{680}.

P. Fromme (*Max-Volmer-Laboratorium für Biophysikalische Chemie und Biochemie, Technische Universität, Berlin, Germany*). I have two questions: (1) I agree strongly with your presentation that protons arising in the medium in the case of intact PSII are not directly released from the Mn cluster but are transferred via several bases, given that the distance of the Mn cluster to the surface is greater that 20 Å. However, direct extraction of a substrate proton by $Y^{\cdot}_Z$ might be difficult. Could you also explain your model with an H-bonding H_2O network?

C. Tommos. Yes, the H-atom abstraction model does not necessarily require direct proton abstraction by the tyrosine radical. The model postulates net proton transfer from the manganese/substrate site to the tyrosine radical. This could occur either directly or via a bridging water molecule.

P. Fromme. (2) Does the pK value really only reflect the pK of a single amino acid or does it reflect (like for Q_B) a network of water and/or bases?

C. Tommos. I think that it is very likely that the pH profiles of both the oxidation and reduction of Y_Z in manganese-depleted PSII reflect global pK values representing a network of amino acids, including His190 and possibly water molecules.

L. Hammarström (*Department of Physical Chemistry, Uppsala University, Uppsala, Sweden*). I wish to make the point that proton movement from reduced Y_Z to water as a base is too slow to explain the experimental data (ΔpK_a is *ca*. 12 between a reduced tyrosine and H_2O). Therefore, Y_Z in its reduced state must be H-bonded to a better base and not to a chain of water molecules.

C. Tommos. The experimental data on Y_Z oxidation in apo-PSII and His190 mutants strongly suggest a tight connection between the tyrosine and the histidine. Personally, I don't think that there is a chain of water molecules between Y_Z and His190, but in the absence of a high-resolution structure of the tyrosine site we can only guess the exact geometry.

C. Zhang (*Department of Biochemistry, Lund University, Lund, Sweden*). How do you explain that the oxidation of Y_Z in apo-PSII is strongly dependent on pH, while with oxygen-evolving PSII this oxidation is pH-independent?

C. Tommos. The pK value of the proton-accepting network is lower in the native enzyme relative to apo-PSII. Measurements of Y_Z oxidation in native PSII set the upper limit of the pK of the base cluster connected to Y_Z in oxygen-evolving PSII to about 4.5 or lower.

S. Styring (*Department of Biochemistry, Lund University, Lund, Sweden*). I wish to comment that we observed oxidation of Y_Z at 5 K in the S_0 and S_1 states. There must therefore be a base present that is well connected to Y_Z in its reduced form. Maybe this base is not His190, as indicated from the recent work from Berlin, but I agree with Dr Hammarström that it is not water so there must be another base present.

A. W. Rutherford (*Service de Bioénergétique, Saclay, France*). I wish to point out that the data on electrochromic band-shifts are pH-independent. The H-release pattern is pH-dependent. These observations are taken to indicate that there is charge accumulation. This therefore suggests that concerted electron–proton transfer or H-abstraction only occurs on the higher S-states.

C. Tommos. The observed optical band-shifts have been interpreted to be of electrochromic origin and to arise from changes in net charge at the active site. The optical band-shift could, however, reflect a change in dipole or a structural change at the active site. Both of these effects may give rise to pH-independent spectral band shifts and pH-dependent proton release.

GLOSSARY

CP: chlorophyll-containing protein
CW: continuous wave
EPR: electron paramagnetic resonance
EMR: electron magnetic resonance
FTIR: Fourier transform infrared
LHCII: light-harvesting complex II
PSII: photosystem II